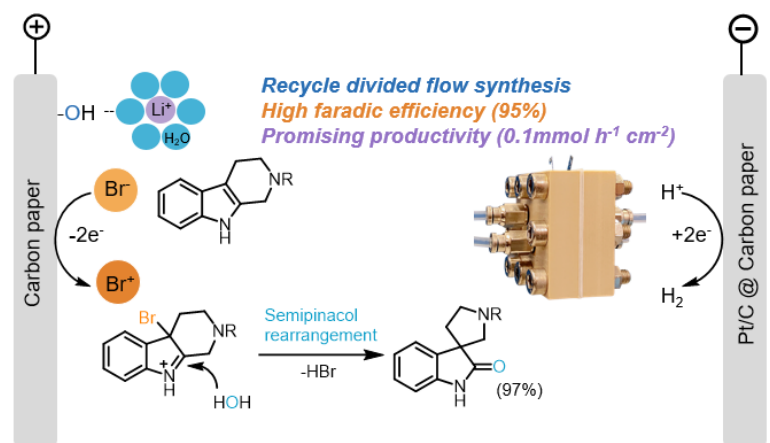


# Electrochemical Oxidative Rearrangement of Tetrahydro- $\beta$ -carbolines in Zero-gap Flow Cell

Yiting Zheng<sup>1,5,6</sup>, Yuen Tsz Cheung<sup>3,6</sup>, Lixin Liang<sup>3</sup>, Huiying Qiu<sup>3</sup>, Terry Tong<sup>1</sup>, Lei Zhang<sup>2</sup>, Anson Tsang<sup>1</sup>, Qing Chen<sup>1,2,3\*</sup> & Rongbiao Tong<sup>3,4\*</sup>

**Abstract:** Oxidative rearrangement of tetrahydro- $\beta$ -carbolines (TH $\beta$ Cs) is one of the most widely used reactions for the synthesis of biologically active spirooxindoles (natural products and drug molecules). While enzymatic and chemical oxidation methods have been well established for this transformation, the corresponding electrochemical approach remain unknown. Herein, we reported the first electrochemical oxidative rearrangement of TH $\beta$ Cs in a zero-gap flow cell. Under the optimal condition, the reaction can afford the desired spirooxindoles with up to 97% yield at a Faradaic efficiency (FE) of 96% and a productivity of 0.144 mmol/(h $\cdot$ cm<sup>2</sup>), which is the best among similar organic electrochemical reactions. Additionally, we discovered lithium ion played a key role in improving the reaction yield.



<sup>1</sup>Department Mechanical and Aerospace Engineering, <sup>2</sup>Energy Institute, <sup>3</sup>Department of Chemistry, and <sup>4</sup>the Southern Marine Science and Engineering Guangdong Laboratory (Guangzhou), The Hong Kong University of Science and Technology, Clear Water Bay, Kowloon, Hong Kong SAR, China. <sup>5</sup>State Key Laboratory of Electrical Insulation and Power Equipment, Xi'an Jiaotong University, Xi'an, 710049, China. <sup>6</sup>These authors contributed equally: Yiting Zheng & Yuen Tsz Cheung. \*email: [chenqing@ust.hk](mailto:chenqing@ust.hk) (Q.C.); [rtong@ust.hk](mailto:rtong@ust.hk) (R. T.)

## Introduction

Oxidative rearrangement of tetrahydro- $\beta$ -carboline (TH $\beta$ Cs)<sup>1</sup> (Figure 1) was proposed as an enzyme-mediated reaction<sup>2-4</sup> responsible for biosynthesis of many biologically active spiro[indolizidine-1,3-oxindole] (i.e., spirooxindoles) natural products such as mitraphylline, rhynchophylline, (iso)corynoxine, corynoxine, corynoxine B, spirotryprostatins A and B, and alstonisine (Figure 1). With chemical oxidants [Pb(OAc)<sub>4</sub>, OsO<sub>4</sub>, *t*-BuOCl, and *N*-bromosuccinimide (NBS), etc] identified for such oxidative rearrangement, it becomes a widely employed method for the construction of spiro[indolizidine-1,3-oxindole],<sup>5-11</sup> which is associated with significant biological activities (antiviral,<sup>12</sup> anticancer,<sup>13</sup> and antibacterial<sup>14</sup>) and regarded as a pharmaceutically privileged structural motif.<sup>15-18</sup> However, these chemical oxidants are hazardous and toxic and would generate stoichiometric amount of harmful chemical waste that poses a significant threat to human health and environment. Recently, our group reported two green protocols that exploited oxone-halide<sup>19</sup> and Fenton-halide<sup>20</sup> for the oxidative rearrangement of TH $\beta$ Cs, which significantly reduce the negative impact on environment and human health.

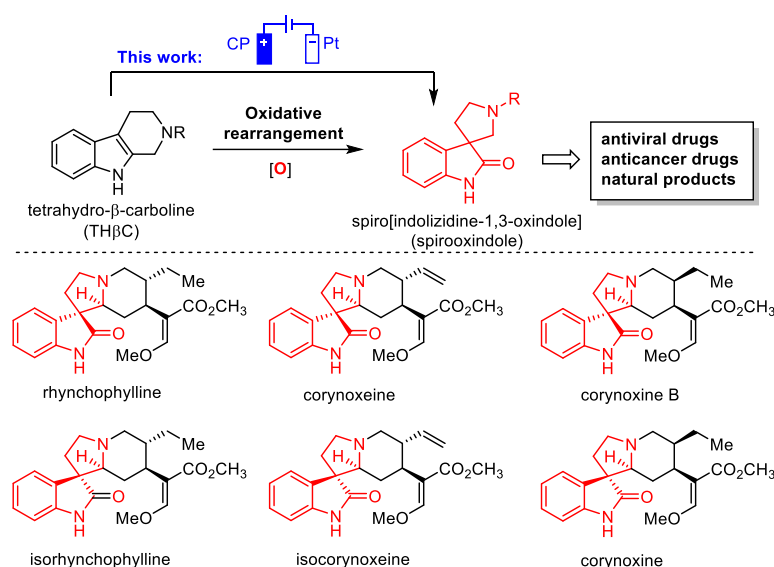


**Figure 1.** Oxidative rearrangement of tetrahydro- $\beta$ -carboline and spirooxindole natural products

To further eliminate oxidants from the reactions, we resort to electrochemistry. Electrochemical synthesis, a potentially sustainable and atom-economic means towards organic compounds, has received increasing attention in the past decade.<sup>21-24</sup> The use of mediators for electro-oxidation/reduction is one of the most effective strategies to achieve high regio- and chemo-selectivity through minimizing the direct non-selective oxidation/reduction of substrates by the electrodes. Halides have emerged as one of the most successful mediators for selective electrochemical organic synthesis.<sup>25</sup> Mechanistically, the halide mediator NaX, KX, NH<sub>4</sub>X or n-Bu<sub>4</sub>NX (X<sup>-</sup> is Cl<sup>-</sup>, Br<sup>-</sup> or I<sup>-</sup>) is oxidized at the anode into reactive halogenating species (RHS), which then reacts with substrates to generate an intermediate that can undergo further transformation(s) to yield the product. Inspired by this general mechanism, we envisioned that the electro-generated RHS could be used as an oxidant for the oxidative rearrangement of TH $\beta$ Cs (Figure 2) because RHS generated *in situ* from chemical oxidation of halide (Oxone/halide or Fenton-halide) was successfully used for this reaction.<sup>19,20</sup> The challenge is the competing nonselective anodic oxidation of TH $\beta$ Cs over halide. Notably, direct electro-oxidation of indoles was reported by Oliveira-Brett,<sup>26</sup> Mount,<sup>27</sup> Vincent,<sup>28,29</sup> Lei,<sup>30</sup> Fang,<sup>31</sup> etc. Therefore, the selective electro-oxidation of halide to RHS in the presence of indoles (i.e., TH $\beta$ Cs) is critical to the success of the oxidative rearrangement of TH $\beta$ Cs.

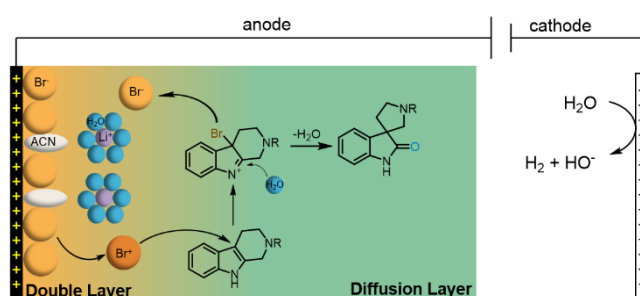


**Figure 2.** Our proposed bromide-mediated electrochemical oxidative rearrangement of tetrahydro- $\beta$ -carboline to spirooxindole

This selectivity challenge permeates into all aspects of the reaction and cell designs

and thus needs both science and engineering to work together. As we illustrate in Figure 2, the challenge begins at the double layer, where the choices of the anode and even the supporting electrolyte can determine if the electrochemical reaction is the generation of RHS or the undesired nonselective oxidation of TH $\beta$ Cs. Away from the double layer enters the diffusion layer, where we desire the rapid transport of the halide towards the electrode for an adequate local concentration of RHS necessary for the rearrangement, while avoiding concentration polarization that may result in side reactions.<sup>32,33</sup> At last, the electrons from the anode must be consumed at the cathode through a sustainable reaction, preferably water splitting without decomposing the reactant or the product from the anode. In our work, we address the challenge with LiBr as the mediator in a zero-gap, high-rate divided flow cell. The synthesis delivers high Faradaic efficiencies and high productivities owing to the rapid mass transports and a beneficial spectator effect of Li<sup>+</sup>. We demonstrate the excellent functional group tolerance with 20 cases of TH $\beta$ Cs oxidative rearrangement into spirooxindoles.

## Results

### Flow cell and condition development

With TH $\beta$ C **1a** as the model compound, we designed the electrochemical synthesis as follows. The electrolyte contained two common solvents: water for high salt solubility and high conductivity, and acetonitrile (MeCN) for dissolving organic molecules. We added acetic acid (AcOH), which was shown to facilitate the generation of RHS in aqueous media.<sup>34</sup> The volume ratio of MeCN, AcOH, and H<sub>2</sub>O was optimized to be 15:2.4:2 (Figure S2). The anode was a commercial carbon paper (CP, SGL-39AA), baked in the air at 400 °C for 24 hours before use to improve wetting with the electrolyte and further suppress oxygen evolution reaction (OER).<sup>35</sup> The cathode was Pt plate for its catalytic activity towards hydrogen evolution reaction (HER). The electrodes were then assembled in a zero-gap flow cell as shown in Figure 3. The term zero-gap refers to the design that the anode, the membrane, and the

cathode were pressed together by two PEEK endplates and sealed with PTFE gaskets. Through a serpentine flow channel engraved in the anode endplate, a peristaltic pump circulated the electrolyte at a relatively fast flow rate (>5 mL/min). Pt foils served as the current leads for applying a fixed potential to the cell for the reaction.

Under the optimal condition (Table 1), the oxidative rearrangement of **1a** achieved a high yield of 97% and a Faradaic efficiency (FE) of 96%. The yield was attained at the approximate point of full conversion as monitored via thin layer chromatography (TLC). The spirooxindole was then isolated from the electrolyte for NMR analysis and a weight measurement. The amount of the product was also converted to charge via Faraday's law, the ratio of which over the charge input during the synthesis was the FE. In comparison, when the reaction was carried out in an undivided cell under otherwise the same condition, the yield and the FE were significantly lower. Issues of the undivided cell will be further discussed in the part of substrate scope.

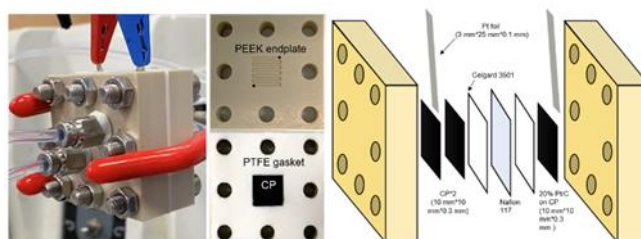
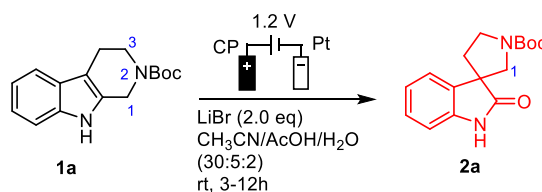


**Figure 3.** Photo of flow cell, endplate, gasket and electrode. Cartoon on the right shows the key components of the cell.

**Table 1.** Selected conditions for bromide-mediated electro-oxidative rearrangement of TH $\beta$ C **1a**.<sup>a</sup>



entry	Deviation from optimized condition	Yield (%) <sup>b</sup>	Faradaic efficiency (%)
1	none	97	96
2	LiBr: 1.2 eq	67	67
3	LiBr: 3.0 eq	88	88
4	Undivided cell	80	68
5	Pt anode	24	9
6	No halide	0	0
7	LiCl instead of LiBr	7	5
8	LiI instead of LiBr	32	7.5
9	E: 0.85 V	55	55
10	E: 1.0 V	71	71
11	E: 1.6 V	50	50

<sup>a</sup>The reaction was carried out at room temperature with anolyte: TH $\beta$ C (0.2 mmol), LiBr (0.4 mmol, 2.0 eq). The reaction was performed in a zero-gap (Nafion 117) flow cell as General Procedure A in SI. <sup>b</sup>NMR yield was obtained.

The impacts of key variables of the reaction design are highlighted in Table 1 with **1a** as the model compound. A variable unique to the electrochemical synthesis is the metal cation. Despite its lack of direct involvement in the reactions, we observed substantial differences in the FE in the order of Li<sup>+</sup> > Na<sup>+</sup> > K<sup>+</sup> > Bu<sub>4</sub>N<sup>+</sup> (as Figure 4c shows). Similar observations had been made in other electrochemical organic syntheses, though not yet explained. We speculate that the cations act as spectators, as broadly discussed in the literature on HER

and OER where the catalytic activities were correlated to the hydration energies of the cations, an indicator of the degree of blockage of active sites at the electrode by the hydrated cations.<sup>36-38</sup> A similar correlation was found between the FE and the hydration energy in our case. The cation effect was less likely on the bromide oxidation as the current density increased along with the hydration energy in Figure 4c. Instead, it was more likely on the side reactions such as the direct oxidation of indole followed by polymerization. In the case of lithium ion ( $\text{Li}^+$ ), its high hydration energy led to a 'water-rich' double layer<sup>36,38</sup> that kept the hydrophobic TH $\beta$ C away from the electrode (present in Figure 2). The interpretation was further supported by the current-time profiles and hydration energy analyses. At the beginning of the reaction, the oxidation current was stable with LiBr, but it decayed quickly with KBr (Figure 4d), which suggested passivation. When examining the carbon paper with scanning electron microscopy (SEM) (the inset of Figure 4d) upon completion of the reaction using KBr, we did find a layer of porous organic matter (derived from side reactions of TH $\beta$ C) in the pristine carbon paper. In contrast, we did not observe similar porous organic matter when LiBr was used. In a control experiment, we also observed a much larger oxidation peak in LSV with KBr than that with LiBr in the supporting electrolyte (see Figure S1a). Although the complex surface of the carbon paper did not permit full elucidation of the spectator effect, our experimental results supported the great impact of cation spectator on organic electrochemical synthesis, which merits future investigations.

The optimal equivalency of bromide ion was determined to be twice of that of TH $\beta$ C because significant OER was observed with 1.2 equivalent of LiBr while aromatic bromination competed effectively with 3.0 equivalent of LiBr (Table 1, entries 2,3). A change of the anode from the carbon paper to Pt mesh (entry 5) diminished the yield and FE drastically, due to side reactions catalyzed by Pt such as the C1 oxidation/ring-opening and/or OER.<sup>39</sup> We also examined other halides ( $\text{Cl}^-$  and  $\text{I}^-$ ) (entries 7,8), but they were not effective mediators. We suspected that the oxidation potential of the chloride ion might be higher than the nonselective

indole oxidation. Although iodide ion can be oxidized at a low oxidation potential into iodonium ion [ $I^+$ ], the iodonium-mediated oxidative rearrangement was slow<sup>40</sup> and consequently nonselective indole oxidation by the electrode at the anode occurred.

The optimal potential was determined to be 1.2 V across the two electrodes: at a lower potential (0.85 and 1.0 V, Table 1, entries 9,10), little or insufficient RHS [ $Br^+$ ] was produced to initiate the rearrangement; while at a higher potential (1.6 V, entry 11), OER and C1 oxidation/ring-opening (side product) were observed. It was corroborated by linear sweeping voltammetry (LSV, Figure 4a). We characterized three electrolytes in a three-electrode cell, a blank supporting electrolyte of 0.8 M  $LiClO_4$ , the supporting electrolyte with TH $\beta$ Cs, and the electrolyte with LiBr. Although the addition of the supporting salt was necessary for the ionic conductivity in the characterization but potentially complicated the reaction mechanism, we could estimate the onset potentials of the reactions in agreement with the selection of optimal potential in the flow cell. The oxidation of bromide ion was about 0.2 V earlier than a small oxidation peak, which was likely associated with the C1 oxidation/ring-opening reaction of TH $\beta$ C and responsible for the low yield when no mediator was used in the flow cell (entry 6). The OER took place at a higher potential. Therefore, the highest efficiency was in a ~0.2 V window.

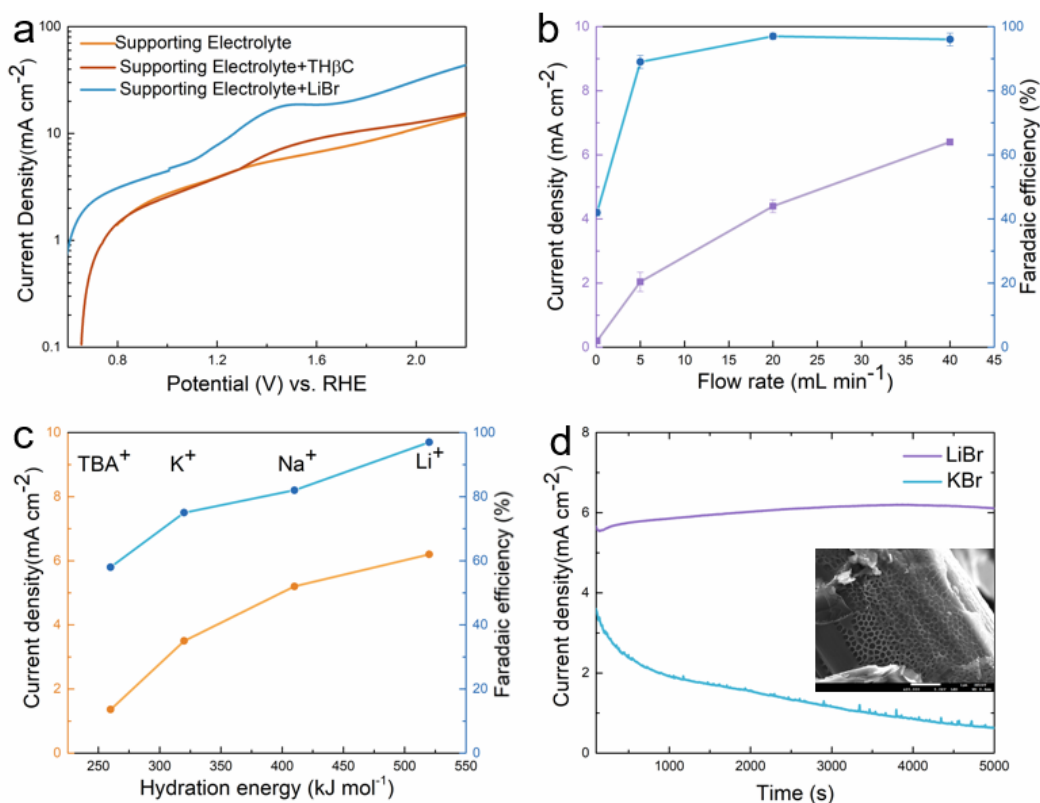


**Figure 4.** The variables of the electro-oxidative rearrangement of THβC. **a** LSV of a supporting electrolyte (0.8 M LiClO<sub>4</sub>, orange), the supporting electrolyte with THβC, and with LiBr. The experiment was conducted in a three-electrode cell as Figure S1 at 50 mV/s. **b** The impact of flow rates on the productivity, the current density (purple), and the FE (blue); **c** The effect of cations on the current density (orange) and the FE (blue). **d** Current-time profiles with LiBr (purple) and KBr (blue) as the salt. The inset is the SEM image of carbon fiber in the carbon paper used in the synthesis reaction with KBr, on which a porous organic layer is likely the polymer product of the side reaction. **b-d** as General Procedure A in SI.

Another key variable is the rate of electrolyte flow. The zero-gap design permits a high flow rate for rapid oxidation of Br<sup>-</sup> despite its relatively low concentration, up ~6 mA/cm<sup>2</sup> at 40 mL/min, translating to ~10% of Br<sup>-</sup> oxidized per pass of flow (Figure 4b). In addition, the FE was increased slightly to 97% with the flow rate, which displayed the other key advantage of rapid flow. As the oxidation of Br<sup>-</sup> was under the limit of mass transport (Figure S1b), the higher flow rate, the more vigorous convective transport, the higher interface concentration of Br<sup>-</sup>, and the more selective the reaction towards the rearrangement. This advantage allowed the flow cell to deliver superior yields over not only the H-cell (Table 1, entry 4 as Figure S4 present), but likely also flow cells that operate at slow flow rates (<1 mL/min in

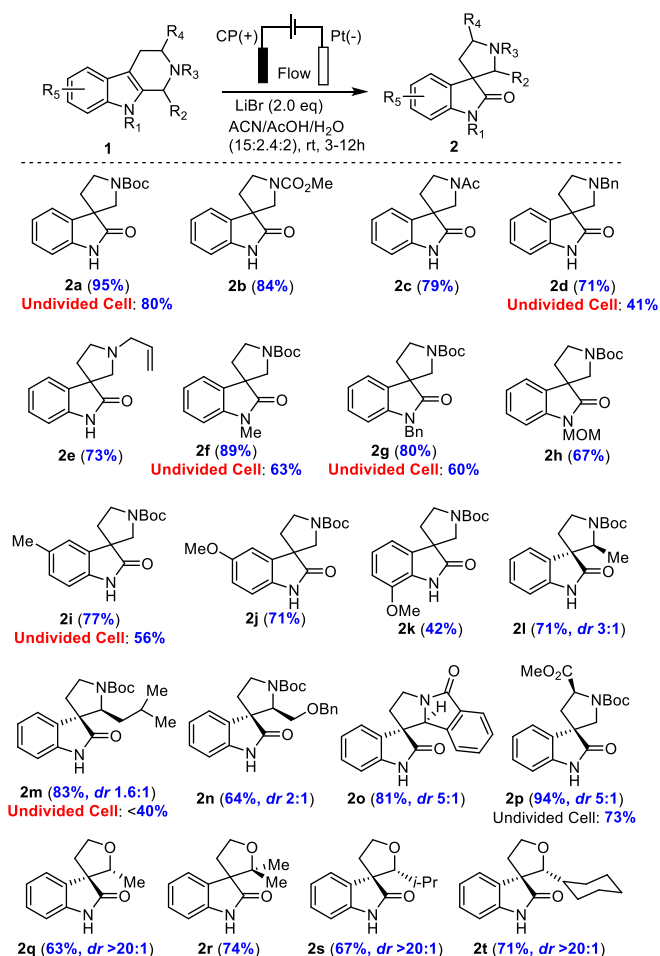
Figure 4b) under single-pass conditions.<sup>44</sup>

### Substrate scope

The substrate scope was investigated, and the results were summarized in Table 2. Comparing to the use of undivided cell in our hand, the yield from the zero-gap flow cell was usually higher (**2a-2e**, **2f-2j**, **2m**, and **2p**). Various N2 protecting groups (NR<sub>3</sub>) including N-CO<sub>2</sub>Me, N-Ac, N-Bn and N-allyl (**2a-2e**) were tolerated in the electrochemical condition with good to excellent yields (71-95%). Notably, N-Bn and N-allyl of TH $\beta$ Cs were suitable substrates for this electrochemical oxidation, which was interesting in light of the well-established Shono oxidation<sup>42,43</sup> that was the major pathway for tertiary amines or amides under conventional electrochemical oxidation conditions. Our studies (Table 2 and Figure 4c) suggested that lithium-ion hydrates might impede the direct Shono oxidation of TH $\beta$ Cs at the anode. This finding was important for mediator-promoted electrochemical oxidation/reduction in organic synthesis and for application of our electrochemical oxidative rearrangement of TH $\beta$ Cs in synthesis of bioactive spirooxindole molecules containing N-alkyl group, especially in tertiary amines. Next, we examined the protecting group on indole nitrogen (NR<sub>1</sub>) and found that only electron-donating groups such N-Me (**2f**), N-Bn (**2g**), and N-MOM (**2h**) were suitable for the oxidative rearrangement with good yields (67-89%), while electron-withdrawing groups (N-Ac, N-Ts, and N-Boc) (not shown) failed. Electron-rich TH $\beta$ Cs with methyl or methoxy group on the benzene ring were good substrates for the electrochemical oxidative rearrangement to provide the spirooxindoles with good yields (**2i-2k**: 42-77%). Different C1 substituents (R<sub>2</sub>) of TH $\beta$ Cs did not reduce considerably the yields (64-83%), but a diastereomeric mixture (**2l-2o**) was often obtained with a ratio ranging from 1.6:1-5:1. Fortunately, these diastereomers could be separated by flash column chromatography on silica gel and assigned reliably by comparison of NMR spectra with reported ones.<sup>19</sup> When tryptophan-derived TH $\beta$ C was used, the spirooxindole (**2p**) was isolated in excellent yield

(94%) under our optimal condition, although diastereoselectivity was only moderate (dr. 5:1). Lastly, we further extended our electrochemical oxidative rearrangement to tetrahydropyrano[3,4-b]indoles (THPIs).<sup>19</sup> All THPIs with monosubstituted or disubstituted alkyl groups at C2 position underwent the expected oxidative rearrangement to provide **2q**-**2t** in good yields. Interestingly, the diastereoselectivity (dr. >20:1) was excellent as compared to TH $\beta$ C substrates. While more TH $\beta$ Cs and THPIs might need to be examined, we were confident that our LiBr-mediated electrochemical oxidative rearrangement provided a green, reliable method for the synthesis of bioactive spirooxindoles.

**Table 2.** Substrate scope of electrochemical oxidative rearrangement of tetrahydro- $\beta$ -carbolines to spirooxindoles<sup>a</sup>.



<sup>a</sup>Condition: the reaction was carried out at room temperature with anolyte: TH $\beta$ C (0.2 mmol), LiBr (0.4 mmol 2.0 eq), as General Procedure A in SI. Isolated yield was obtained.

Finally, we compared our results with other electrochemical oxidation reactions, in particular, of indole or related N-heterocycle compounds<sup>44-49</sup> in Figure 5 (also see Tables S2-3), which include: (a) electrochemical 1,2-diarylation<sup>44</sup> of alkenes with a  $\text{CoCl}_2$  catalyst; (b) electrochemical diazidation<sup>45</sup> reaction of alkenes with the  $\text{MnBr}_2$  catalyst; (c) electro-oxidative [3+2] annulation<sup>46</sup> of phenol and indole; (d) electrochemical radical cascade cyclization<sup>47</sup> of N-methacryloyl-2-phenylbenzimidazole and alkyl boronic acid; (e) electrochemical flow microreactor<sup>48</sup> for efficient synthesis of isoquinoline-6(5H)-ones; and (f) flow Rhodaelectrocatalyzed alkyne annulations<sup>49</sup>. They were compared with ours in terms of the yield and productivity, i.e., the amount of the desired product per unit of reaction time and per area of the cell [in  $\mu\text{mol}/(\text{h}\cdot\text{cm}^2)$ ]. The higher productivity, the shorter time and the smaller cell required, the more cost-effective. As shown in Figure 5, the yield (**2p**, 94%) of our reaction system was among the best, while the productivity (**2p**,  $144 \mu\text{mol}/(\text{h}\cdot\text{cm}^2)$ ) (also see Table S3 in Supporting Information) was much higher than all other electrochemical reactions. We attributed our outstanding performance to the following two factors: 1) the zero-gap flow cell minimizes the overpotential and mitigates the trade-off between a high current and a high selectivity, which is typically encountered in a cell with less forced convection; and 2) the use of bifunctional mediator LiBr with a suitable oxidation potential leaves a sufficiently wide potential window for the high selectivity.

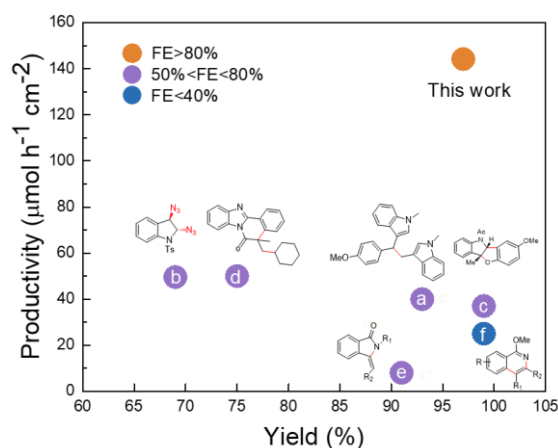


**Figure 5.** Comparison of productivity, Faradaic efficiencies and yield cycle life (Noted: all selected electro-oxidation of indole or N-heterocyclic compounds for a fair comparison, Table S3 summarizes the detail calculation; red bond represents new generated bond during the electrochemical reaction)<sup>44-49</sup>

## Conclusion

We have designed a zero-gap flow cell and demonstrated efficient, high-rate LiBr-mediated electro-oxidative rearrangement of tetrahydro- $\beta$ -carbolines to spirooxindoles using commercial electrodes. The generality of this electrochemical oxidative rearrangement was demonstrated with 20 examples with good to excellent yields. Importantly, we discovered that the lithium ion played a key role as a spectator in the double layer to suppress the direct oxidation of the substrate and improve the yield. Compared to other electrochemical reactions reported in the recent literature, our designed zero-gap flow cell delivers the highest Faradaic efficiency and productivity. We expect that our catalytic system and cell design could be further applied to other electro-organic reactions.

## Methods

**Oxidative rearrangement of TH $\beta$ Cs (General Procedure A):** Reactions were conducted in two 20 mL vials with anolyte and catholyte. A carbon paper (10 mm\*10 mm\*0.6 mm) working electrode (anode) and a 20% Pt/graphite carbon paper (10 mm\*10 mm\*0.3 mm). The reaction was performed in the two PEEK housing zero-gap (Nafion 117) flow cell at constant voltage 1.2 V with PTFE gasket and celgard 3501. To a solution of TH $\beta$ Cs (0.2 mmol) in MeCN/AcOH/H<sub>2</sub>O (15:2.4:2, 10 mL) at anode was added bromide salt (0.4 mmol, 2.0 equiv.). This electrolyte was separated from the cathode electrolyte in H<sub>2</sub>SO<sub>4</sub> (0.25M, 10 mL) by a proton-exchange membrane Nafion 117 (12 mm\* 12 mm, pre-treatment with MeCN). The constant potential 1.2 V and 20 mL/min were set for synthesis, and the cut-off charge was set 2 F/mol. Reaction was monitored by TLC. The reaction mixture was diluted with EtOAc (10 mL). Saturated aqueous Na<sub>2</sub>CO<sub>3</sub> solution (10 mL) was added. The organic fraction was

collected, and the aqueous fraction was extracted with EtOAc (2 x 10 mL). The combined organic fraction was washed with brine, dried over Na<sub>2</sub>SO<sub>4</sub>, filtered and concentrated under reduced pressure. The resulting residue was purified by flash column chromatography on silica gel using hexane/ethyl acetate eluents.

### Data availability

The authors declare that all relevant data supporting the findings of this study are available within the article and its Supplementary Information files.

### References

- 1 Finch, N. & Taylor, W. I. The Conversion of Tetrahydro- $\beta$ -Carboline Alkaloids into Oxindoles. the Structures and Partial Syntheses of Mitrephylline and Rhyncophylline. *J. Am. Chem. Soc.* **84**, 1318-1320 (1962).
- 2 Liu, Z. *et al.* Structural basis of the stereoselective formation of the spirooxindole ring in the biosynthesis of citrinadins. *Nat Commun* **12**, 4158 (2021).
- 3 Szabo, L. F. Rigorous biogenetic network for a group of indole alkaloids derived from strictosidine. *Molecules* **13**, 1875-1896 (2008).
- 4 O'Connor, S. E. & Maresh, J. J. Chemistry and biology of monoterpene indole alkaloid biosynthesis. *Nat. Prod. Rep.* **23**, 532-547 (2006).
- 5 Edmondson, S. D. & Danishefsky, S. J. The total synthesis of spirotryprostatin A. *Angew. Chem. Int. Ed.* **37**, 1138-1140 (1998).
- 6 Edmondson, S., Danishefsky, S. J., Sepp-Lorenzino, L. & Rosen, N. Total synthesis of spirotryprostatin A, leading to the discovery of some biologically promising analogues. *J. Am. Chem. Soc.* **121**, 2147-2155 (1999).

- 7 von Nussbaum, F. & Danishefsky, S. J. A rapid total synthesis of spirotryprostatin B: Proof of its relative and absolute stereochemistry. *Angew. Chem. Int. Ed.* **39**, 2175-2178 (2000).
- 8 Ito, M., Clark, C. W., Mortimore, M., Goh, J. B. & Martin, S. F. Biogenetically inspired approach to the Strychnos alkaloids. Concise syntheses of (+/-)-akuammicine and (+/-)-strychnine. *J. Am. Chem. Soc.* **123**, 8003-8010 (2001).
- 9 Takayama, H., Fujiwara, R., Kasai, Y., Kitajima, M. & Aimi, N. First asymmetric total synthesis of Us-7 and-8, novel D-seco corynanthe-type oxindole alkaloids from *Uncaria attenuata*: Structure revision of Us-7 and determination of absolute stereochemistry. *Org. Lett.* **5**, 2967-2970 (2003).
- 10 Martin, S. F., Benage, B., Geraci, L. S., Hunter, J. E. & Mortimore, M. Unified Strategy for Synthesis of Indole and 2-Oxindole Alkaloids. *J. Am. Chem. Soc.* **113**, 6161-6171 (1991).
- 11 Marti, C. & Carreira, E. M. Construction of spiro[pyrrolidine-3,3'-oxindoles] - Recent applications to the synthesis of oxindole alkaloids. *Eur. J. Org. Chem.* **2003**, 2209-2219 (2003).
- 12 Ye, N., Chen, H., Wold, E. A., Shi, P.-Y. & Zhou, J. Therapeutic Potential of Spirooxindoles as Antiviral Agents. *ACS Infect. Dis.* **2**, 382-392 (2016).
- 13 Zhao, Y. *et al.* A Potent Small-Molecule Inhibitor of the MDM2-p53 Interaction (MI-888) Achieved Complete and Durable Tumor Regression in Mice. *J. Med. Chem.* **56**, 5553-5561 (2013).
- 14 Bhaskar, G., Arun, Y., Balachandran, C., Saikumar, C. & Perumal, P. T. Synthesis of novel spirooxindole derivatives by one pot multicomponent reaction and their antimicrobial activity. *Eur. J. Med. Chem.* **51**, 79-91 (2012).

- 15 Panda, S. S., Jones, R. A., Bachawala, P. & Mohapatra, P. P. Spirooxindoles as Potential Pharmacophores. *Mini-Reviews in Medicinal Chemistry* **17**, 1515-1536 (2017).
- 16 Zhou, L.-M., Qu, R.-Y. & Yang, G.-F. An overview of spirooxindole as a promising scaffold for novel drug discovery. *Expert Opinion on Drug Discovery* **15**, 603-625 (2020).
- 17 Galliford, C. V. & Scheidt, K. A. Pyrrolidiny-Spirooxindole Natural Products as Inspirations for the Development of Potential Therapeutic Agents. *Angew. Chem. Int. Ed.* **46**, 8748-8758 (2007).
- 18 Yu, B., Yu, D.-Q. & Liu, H.-M. Spirooxindoles: Promising scaffolds for anticancer agents. *Eur. J. Med. Chem.* **97**, 673-698 (2015).
- 19 Xu, J., Liang, L. X., Zheng, H. H., Chi, Y. G. R. & Tong, R. B. Green oxidation of indoles using halide catalysis. *Nat Commun* **10**, 4754 (2019).
- 20 Zhao, G. D. *et al.* Fenton chemistry enables the catalytic oxidative rearrangement of indoles using hydrogen peroxide. *Green Chem.* **23**, 2300-2307 (2021).
- 21 Yan, M., Kawamata, Y. & Baran, P. S. Synthetic Organic Electrochemical Methods Since 2000: On the Verge of a Renaissance. *Chem. Rev.* **117**, 13230-13319 (2017).
- 22 Kärkäs, M. D. Electrochemical strategies for C–H functionalization and C–N bond formation. *Chem. Soc. Rev.* **47**, 5786-5865 (2018).
- 23 Moeller, K. D. Using Physical Organic Chemistry To Shape the Course of Electrochemical Reactions. *Chem. Rev.* **118**, 4817-4833 (2018).
- 24 Waldvogel, S. R., Lips, S., Selt, M., Riehl, B. & Kampf, C. J. Electrochemical Arylation Reaction. *Chem. Rev.* **118**, 6706-6765 (2018).
- 25 Tang, H.-T., Jia, J.-S. & Pan, Y.-M. Halogen-mediated electrochemical organic synthesis. *Org. Biomol. Chem.* **18**, 5315-5333 (2020).

- 26 Enache, T. A. & Oliveira-Brett, A. M. Pathways of Electrochemical Oxidation of Indolic Compounds. *Electroanalysis* **23**, 1337-1344 (2011).
- 27 Jennings, P., Jones, A. C., Mount, A. R. & Thomson, A. D. Electrooxidation of 5-substituted indoles. *J. Chem. Soc., Faraday Trans.* **93**, 3791-3797 (1997).
- 28 Wu, J., Dou, Y., Guillot, R., Kouklovsky, C. & Vincent, G. Electrochemical Dearomative 2,3-Difunctionalization of Indoles. *J. Am. Chem. Soc.* **141**, 2832-2837 (2019).
- 29 Vincent, G., Abou-Hamdan, H. & Kouklovsky, C. Dearomatization Reactions of Indoles to Access 3D Indoline Structures. *Synlett* **31**, 1775-1788 (2020).
- 30 Liu, K. *et al.* Electrooxidation enables highly regioselective dearomative annulation of indole and benzofuran derivatives. *Nat Commun* **11**, 3 (2020).
- 31 Qin, H. *et al.* An Electrochemical Route for Special Oxidative Ring-Opening of Indoles. *Chem. Eur. J.* **27**, 13024-13028 (2021).
- 32 Jebaraj, A. J. J., Georgescu, N. S. & Scherson, D. A. Oxygen and Hydrogen Peroxide Reduction on Polycrystalline Platinum in Acid Electrolytes: Effects of Bromide Adsorption. *J. Phys. Chem. C* **120**, 16090-16099 (2016).
- 33 Zolfaghari, A., Conway, B. E. & Jerkiewicz, G. Elucidation of the effects of competitive adsorption of Cl<sup>-</sup> and Br<sup>-</sup> ions on the initial stages of Pt surface oxidation by means of electrochemical nanogravimetry. *Electrochim. Acta* **47**, 1173-1187 (2002).
- 34 Butler, A. Vanadium haloperoxidases. *Curr. Opin. Chem. Biol.* **2**, 279-285 (1998).
- 35 Chen, Q., Gerhardt, M. R., Hartle, L. & Aziz, M. J. A Quinone-Bromide Flow Battery with 1 W/cm<sup>2</sup> Power Density. *J. Electrochem. Soc.* **163**, A5010-A5013 (2016).
- 36 Subbaraman, R. *et al.* Enhancing Hydrogen Evolution Activity in Water Splitting by Tailoring Li<sup>+</sup>-Ni(OH)<sub>2</sub>-Pt Interfaces. *Science* **334**, 1256-1260 (2011).
- 37 Strmcnik, D. *et al.* The role of non-covalent interactions in electrocatalytic fuel-cell reactions on platinum. *Nat Chem* **1**, 466-472 (2009).

- 38 Stoffelsma, C. *et al.* Promotion of the Oxidation of Carbon Monoxide at Stepped Platinum Single-Crystal Electrodes in Alkaline Media by Lithium and Beryllium Cations. *J. Am. Chem. Soc.* **132**, 16127-16133 (2010).
- 39 Jebaraj, A. J. J., Georgescu, N. S. & Scherson, D. A. Oxygen and Hydrogen Peroxide Reduction on Polycrystalline Platinum in Acid Electrolytes: Effects of Bromide Adsorption. *J. Phys. Chem. C* **120**, 16090-16099 (2016).
- 40 Qian, C., Li, P. & Sun, J. Catalytic Enantioselective Synthesis of Spirooxindoles by Oxidative Rearrangement of Indoles. *Angew. Chem. Int. Ed.* **60**, 5871-5875 (2021).
- 41 Hammerich, O. & Lund, H. *Organic Electrochemistry*. (CRC Press, Taylor & Francis Group, 2000).
- 42 Yamamoto, K., Kuriyama, M. & Onomura, O. Shono - type Oxidation for Functionalization of N-Heterocycles. *Chem. Rec.* **21**, 2239-2253 (2021).
- 43 Yamamoto, K., Kuriyama, M. & Onomura, O. Anodic Oxidation for the Stereoselective Synthesis of Heterocycles. *Acc. Chem. Res.* **53**, 105-120 (2020).
- 44 Qin, J. H., Luo, M. J., An, D. L. & Li, J. H. Electrochemical 1,2-Diarylation of Alkenes Enabled by Direct Dual C-H Functionalizations of Electron-Rich Aromatic Hydrocarbons. *Angew. Chem. Int. Ed.* **60**, 1861-1868 (2021).
- 45 Fu, N. K., Sauer, G. S., Saha, A., Loo, A. & Lin, S. Metal-catalyzed electrochemical diazidation of alkenes. *Science* **357**, 575-579 (2017).
- 46 Liu, K., Tang, S., Huang, P. F. & Lei, A. W. External oxidant-free electrooxidative [3+2] annulation between phenol and indole derivatives. *Nat Commun* **8**, 775 (2017).
- 47 Yuan, Y. *et al.* Mn-Catalyzed Electrochemical Radical Cascade Cyclization toward the Synthesis of Benzo[4,5]imidazo[2,1-a]isoquinolin-6(5H)-one Derivatives. *ACS Catal* **10**, 6676-6681 (2020).

- 48 Folgueiras-Amador, A. A., Philipps, K., Guilbaud, S., Poelakker, J. & Wirth, T. An Easy-to-Machine Electrochemical Flow Microreactor: Efficient Synthesis of Isoindolinone and Flow Functionalization. *Angew. Chem. Int. Ed.* **56**, 15446-15450 (2017).
- 49 Kong, W. J. *et al.* Flow Rhodaelectro-Catalyzed Alkyne Annulations by Versatile C-H Activation: Mechanistic Support for Rhodium(III/IV). *J. Am. Chem. Soc.* **141**, 17198-17206 (2019).

## Acknowledgements

This research was financially supported by the Southern Marine Science and Engineering Guangdong Laboratory (Guangzhou) (SMSEGL20Sc01-B), Research Grant Council of Hong Kong (C6026-19G, 16307219, 16304618, 16306920), the National Foundation of Natural Science, China (52022002), the Electrical Insulation and Power Equipment in Xi'an Jiaotong University and State Key Laboratory (Grant No. EIPE21205). Authors thank for the technical assistance from Fanny and Alex in Materials Characterization and Preparation Facilities (MCPF) in HKUST.

## Author contributions

R.T. and Q.C. conceived and designed the project and wrote the paper with assistance from Y.Z. and Y.T.C.; Y.Z. and Y.T.C. performed the experiments. L.L. performed part of the experiments. H.Q. prepared some related substrates. L.Z. gave the assistance on mechanism study. A.T. gave the assistance in modification of flow cell. All authors discussed the results and commented on the manuscript.

## Additional information

**Supplementary Information** accompanies this manuscript.

**Competing financial interests:** The authors declare no competing financial interests.